Coherent control of multiphoton resonance dynamics in high-order-harmonic generation driven by two frequency-comb fields

Di Zhao,* Chen-Wei Jiang, and Fu-li Li
Department of Applied Physics, School of Science, Xi'an Jiaotong University, Xi'an 710049, China
(Received 18 May 2015; revised manuscript received 1 August 2015; published 14 October 2015)

We present a theoretical investigation of the multiphoton resonance dynamics in the high-order-harmonic generation (HHG) process driven by two frequency-comb fields with the carrier frequencies of fundamental and second harmonics, respectively. The many-mode Floquet theorem is employed to provide a nonperturbative and exact treatment of the interaction between a quantum system and frequency-comb laser fields. The coupling of the weak second-harmonic control frequency-comb laser field promises more routes to coherently optimize the multiphoton resonance dynamics and HHG power spectra. First, even-order harmonics are generated due to the coupling of the second-harmonic frequency-comb field. Second, the HHG power spectra can be greatly enhanced via multiphoton resonance, which can be achieved by tuning the carrier-envelope-phase (CEP) shifts and the peak intensities of both frequency-comb fields. Furthermore, besides the multiphoton transitions involving only fundamental-harmonic photons, additional multiphoton transitions involving both fundamental- and second-harmonic photons occur, resulting in the generation of combs with frequencies dependent on CEP shifts of both fields. Different multiphoton transition paths can interfere with each other when the two CEP shifts are matching, and the interference of paths allows one to coherently control the HHG power spectra by varying the relative phase between the fields.

DOI: 10.1103/PhysRevA.92.043413 PACS number(s): 32.80.Qk, 42.65.Ky, 42.50.Hz

I. INTRODUCTION

Advancements of the phase-stabilized optical frequency comb from a femtosecond laser have remarkably impacted on high-precision optical frequency spectroscopy [1–5], determination of fundamental constants [6,7], testing of quantum electrodynamics [8–11], and development of an optical atomic clock [12–17]. The optical frequency comb can precisely and directly link optical and microwave frequencies [18,19], providing a "ruler" with which an unknown optical frequency can be measured. Generation of frequency combs in the extreme ultraviolet (XUV) and vacuum ultraviolet (VUV) spectral region is highly desirable due to the lack of powerful continuous-wave lasers in those spectral regions.

Coherent XUV [20] and VUV [21] radiations at a repetition frequency of more than 100 MHz have been generated via high-order-harmonic generation (HHG) with a 1000-fold improvement over previous experiments. Additionally, Cingöz *et al.* [22] reported the generation of XUV frequency combs up to the 27th harmonic order (wavelength of 40 nm) by coupling a high-power near-infrared frequency comb to a robust femtosecond enhancement cavity. Theoretical and experimental works [9,22–25] indicate that the frequency-comb structure and coherence can indeed survive in very high-order harmonics and in the presence of substantial ionization. In detail, Son and Chu [26] presented a theoretical nonperturbative investigation for the coherent control of multiphoton resonance dynamics driven by intense frequency-comb laser fields by employing an extension of the many-mode Floquet theory (MMFT) [27–31]. They showed that HHG driven by an intense frequency-comb laser field has a comb structure with the same repetition frequency and different offset frequencies for each harmonic.

The potential applications of frequency-comb structure require the optimization and coherent control of the multiphoton resonance dynamics in the HHG process. One of the optimization goals is the extension of the frequency-comb structure in the HHG power spectra. When only one fundamental frequency-comb laser field is employed, the generated frequency-comb structure is limited to odd-order harmonics due to the inversion symmetry. The generation of frequency-comb structure in even-order harmonics would be valuable for potential applications, such as high-precision optical frequency spectroscopy [1–5]. Another optimization goal is the enhancement of frequency-comb elements in harmonics. Son and Chu have shown that HHG of a two-level system driven by a frequency-comb field can be enhanced via multiphoton resonance by tuning the carrier-envelope phase (CEP) shift of the driving field [26]. Additionally, this multiphoton-resonant-enhancement method has been demonstrated by an *ab initio* theoretical investigation of atomic hydrogen driven by an intense frequency-comb laser field [32], whereas the generation and coherent control of combs with the power per comb element as high as possible are always desired.

In this paper, we present a theoretical investigation of the multiphoton resonance dynamics driven by an intense fundamental-harmonic driving frequency-comb field combined with a weak second-harmonic control frequency-comb field. In the combination field, there are two types of multiphoton transition processes: the one involving only fundamental-harmonic photons gives rise to comb elements in odd-order harmonics; and the other one involving both fundamental- and second-harmonic photons gives rise to comb elements, whose absolute frequencies are dependent on CEP shifts of both fields, in odd- and even-order harmonics. The coupling of the weak control field not only promises the extension of frequency-comb structure to even-order harmonics but also provides more routes to coherently control the multiphoton-

*d.zhao@mail.xjtu.edu.cn

resonance processes for the enhancement of frequency-comb elements in the HHG power spectrum. Our investigation shows that, besides tuning the CEP shift of the fundamental driving field, the multiphoton resonant enhancement of HHG power spectra can be alternatively achieved by varying the peak intensity and CEP shift of the weak control frequency-comb field. In particular, different multiphoton transition paths can be superpositioned via matching CEP shifts of the fields, and the interference of paths allows the coherent control of multiphoton resonance dynamics by varying the relative phase between the fields.

The paper is organized as follows. In Sec. II, we present the MMFT for the treatment of the interaction between finite-level quantum systems and two frequency-comb laser fields with different carrier frequencies and the same repetition frequency. In Sec. III, we apply the MMFT to study the coherent control of multiphoton-resonant dynamics and HHG power spectra of two-level systems. This is followed by the conclusion in Sec. IV.

II. MMFT TREATMENT OF MULTIPHOTON EXCITATION DRIVEN BY INTENSE FREQUENCY-COMB LASER FIELDS

A frequency-comb laser field can be generated by a train of equal-spacing laser pulses, which is written in the form

$$E_f(t) = \sum_n f(t - n\tau) e^{i(\omega_c t - n\omega_c \tau + n\Delta\phi)} + \text{c.c.}, \tag{1}$$

where ω_c is the carrier frequency, τ is the time interval between pulses, $\Delta\phi$ is the carrier-envelope-phase shift from pulse to pulse, $f(t) = f_0 e^{-t^2/2\sigma^2}$ is the envelope function for each pulse, f_0 is the peak amplitude, and σ is the standard deviation of a Gaussian function. Equation (1) can be rewritten as the summation of components of discrete comb frequencies [26,32,33]:

$$E_f(t) = \sum_{k=-\infty}^{\infty} E_k e^{i\omega_k t} + \text{c.c.} \simeq \sum_{k=-N}^{N} E_k e^{i\omega_k t} + \text{c.c.} \tag{2}$$

In Eq. (2), the comb frequencies ω_k can be expressed as [26]

$$\omega_k = \omega_0 + k\omega_r \tag{3}$$

with the repetition frequency $\omega_r = 2\pi/\tau$ and the main angular frequency

$$\omega_0 = \left[\frac{\omega_c - \omega_\delta}{\omega_r}\right]\omega_r + \omega_\delta, \tag{4}$$

where [ ] is the round function and $\omega_\delta = \Delta\phi/\tau$ is the offset frequency. Individual amplitudes of frequencies ω_k are given by

$$E_k = \frac{f_0 \sigma \omega_r}{\sqrt{2\pi}} e^{-\sigma^2(\omega_0 - \omega_c + k\omega_r)/2}. \tag{5}$$

A finite integer number N is chosen to approximately reproduce the frequency-comb field to make sure the calculation is accessible and convergent. In our calculation, N is chosen such that $E_k < 1 \times 10^{-15}$ a.u. (corresponding to peak intensity 3.51×10^{-14} W cm^{-2}) when $|k| > N$.

We consider a quantum system driven by two frequency-comb laser fields, which have the same repetition frequency ω_r. The carrier frequency, main angular frequency, and offset frequency of the first frequency-comb field are ω_c, ω_0, and ω_δ, respectively. And those of the second frequency-comb field are Ω_c, Ω_0, and ω'_δ, respectively. The total electric field can be expressed as

$$E_t(t) = \sum_{k=-N}^{N} E_k e^{i\omega_k t} + \sum_{k=-N'}^{N'} E'_k e^{i\Omega_k t} + \text{c.c.}, \tag{6}$$

in which E_k and E'_k are the amplitudes of frequency components $\omega_k = \omega_0 + k\omega_r$ and $\Omega_k = \Omega_0 + k\omega_r$, respectively. Then the Hamiltonian is given by

$$\begin{aligned}\hat{H}(\mathbf{r},t) &= \hat{H}_0(\mathbf{r}) - \sum_{k=-N}^{N} \mu(\mathbf{r}) \cdot \mathbf{E}_k \cos\omega_k t \\ &\quad - \sum_{k=-N'}^{N'} \mu(\mathbf{r}) \cdot \mathbf{E}'_k \cos\Omega_k t \\ &= \hat{H}_0(\mathbf{r}) - \sum_{k=-N}^{N} \frac{1}{2}\mu_z E_k [e^{i(\omega_0 + k\omega_r)t} + e^{-i(\omega_0 + k\omega_r)t}] \\ &\quad - \sum_{k=-N'}^{N'} \frac{1}{2}\mu_z E'_k [e^{i(\Omega_0 + k\omega_r)t} + e^{-i(\Omega_0 + k\omega_r)t}],\end{aligned} \tag{7}$$

where $\hat{H}_0(\mathbf{r})$ is the unperturbed Hamiltonian of the atomic or molecular system, $\mu(\mathbf{r})$ is the electric dipole moment operator, and μ_z is the component parallel to the polarization axis. Note that the time-dependent Hamiltonian is trichromatic, containing three independent frequencies ω_0, Ω_0, and ω_r.

The many-mode Floquet theory [27–29] can be applied to solve the polychromatic or quasiperiodic time-dependent Schrödinger equation with the Hamiltonian (7), which is converted into an equivalent time-independent generalized Floquet matrix eigenvalue problem. Since all the comb frequencies can be represented by three variables, ω_0, Ω_0, and ω_r, the basis vectors in the three-mode Floquet formalism

$$|\alpha l n m\rangle = |\alpha\rangle \otimes |l\rangle \otimes |n\rangle \otimes |m\rangle \tag{8}$$

are employed. α is the system index, while l, m, and n correspond to Fourier components of ω_0, Ω_0, and ω_r, respectively. Then the time-independent generalized Floquet matrix, in the representation spanned by the basis vectors $\{|\alpha l n m\rangle\}$, has the following explicit form:

$$\sum_\beta \sum_{l'} \sum_{n'} \sum_{m'} \langle \alpha l n m | H_F | \beta l' n' m' \rangle \langle \beta l' n' m' | \lambda \rangle = \lambda \langle \alpha l n m | \lambda \rangle, \tag{9}$$

where λ is the quasienergy eigenvalue and $|\lambda\rangle$ is the corresponding eigenvector.

The Floquet matrix H_F is constructed by

$$\begin{aligned}&\langle \alpha l n m | H_F | \beta l' n' m' \rangle \\ &\quad = H_{\alpha\beta}^{[l-l', n-n', m-m']} + (l\omega_0 + n\Omega_0 + m\omega_r)\delta_{\alpha,\beta}\delta_{l,l'}\delta_{n,n'}\delta_{m,m'},\end{aligned} \tag{10}$$

where

$$H_{\alpha,\beta}^{[l-l',n-n',m-m']} = \varepsilon_\alpha \delta_{\alpha,\beta}\delta_{l,l'}\delta_{n,n'}\delta_{m,m'} + \sum_{k=-N}^{N} V_{\alpha,\beta}^{(k)}\delta_{n,n'}(\delta_{l+1,l'}\delta_{m+k,m'} + \delta_{l-1,l'}\delta_{m-k,m'}) + \sum_{k=-N'}^{N'} U_{\alpha,\beta}^{(k)}\delta_{l,l'}(\delta_{n+1,n'}\delta_{m+k,m'} + \delta_{n-1,n'}\delta_{m-k,m'}), \tag{11}$$

and $\varepsilon_\alpha = \langle\alpha|\hat{H}_0|\alpha\rangle$, $V_{\alpha,\beta}^{(k)} = -\frac{1}{2}E_k\langle\alpha|\mu_z|\beta\rangle$, and $U_{\alpha,\beta}^{(k)} = -\frac{1}{2}E_k'\langle\alpha|\mu_z|\beta\rangle$. Note that the energy $\varepsilon_\alpha + l\omega_0 + n\Omega + m\omega_r$ for each diagonal element in the Floquet matrix H_F is unique, to make sure the issue of degeneracy is avoided. The structure of H_F for the linearly polarized case is as follows:

$$H_F = \begin{pmatrix} \ddots & & & & & \vdots & \\ & A+2\Omega_0 I & B & 0 & 0 & 0 & \cdots \\ & B^T & A+\Omega_0 I & B & 0 & 0 & \\ & 0 & B^T & A & B & 0 & \\ & 0 & 0 & B^T & A-\Omega_0 I & B & \\ \cdots & 0 & 0 & 0 & B^T & A-2\Omega_0 I & \\ & \vdots & & & & & \ddots \end{pmatrix}, \tag{12}$$

where

$$A = \begin{pmatrix} \ddots & & & & & \vdots & \\ & C+2\omega_0 I & X & 0 & 0 & 0 & \cdots \\ & X & C+\omega_0 I & X & 0 & 0 & \\ & 0 & X & C & X & 0 & \\ & 0 & 0 & X & C-\omega_0 I & X & \\ \cdots & 0 & 0 & 0 & X & C-2\omega_0 I & \\ & \vdots & & & & & \ddots \end{pmatrix}, \tag{13}$$

$$B = \begin{pmatrix} \ddots & & & & & \vdots & \\ & X' & 0 & 0 & 0 & 0 & \cdots \\ & 0 & X' & 0 & 0 & 0 & \\ & 0 & 0 & X' & 0 & 0 & \\ & 0 & 0 & 0 & X' & 0 & \\ \cdots & 0 & 0 & 0 & 0 & X' & \\ & \vdots & & & & & \ddots \end{pmatrix}, \tag{14}$$

$$C = \begin{pmatrix} \ddots & & & & & \vdots & \\ & Z+2\omega_r I & 0 & 0 & 0 & 0 & \cdots \\ & 0 & Z+\omega_r I & 0 & 0 & 0 & \\ & 0 & 0 & Z & 0 & 0 & \\ & 0 & 0 & 0 & Z-\omega_r I & 0 & \\ \cdots & 0 & 0 & 0 & 0 & Z-2\omega_r I & \\ & \vdots & & & & & \ddots \end{pmatrix}, \tag{15}$$

$$X = \begin{pmatrix} \ddots & & & & & \vdots & \\ & Y_0 & Y_1 & Y_2 & Y_3 & Y_4 & \cdots \\ & Y_{-1} & Y_0 & Y_1 & Y_2 & Y_3 & \\ & Y_{-2} & Y_{-1} & Y_0 & Y_1 & Y_2 & \\ & Y_{-3} & Y_{-2} & Y_{-1} & Y_0 & Y_1 & \\ \cdots & Y_{-4} & Y_{-3} & Y_{-2} & Y_{-1} & Y_0 & \\ & \vdots & & & & & \ddots \end{pmatrix}, \tag{16}$$

$$X' = \begin{pmatrix} \ddots & & & & \vdots & \\ & Y'_0 & Y'_1 & Y'_2 & Y'_3 & Y'_4 & \cdots \\ & Y'_{-1} & Y'_0 & Y'_1 & Y'_2 & Y'_3 & \\ & Y'_{-2} & Y'_{-1} & Y'_0 & Y'_1 & Y'_2 & \\ & Y'_{-3} & Y'_{-2} & Y'_{-1} & Y'_0 & Y'_1 & \\ \cdots & Y'_{-4} & Y'_{-3} & Y'_{-2} & Y'_{-1} & Y'_0 & \\ & \vdots & & & & & \ddots \end{pmatrix}. \tag{17}$$

The matrices of Y_k, Y'_k, and Z have the following forms:

$$Y_k = \begin{pmatrix} 0 & V^{(k)}_{\alpha\beta} & V^{(k)}_{\alpha\gamma} & \cdots \\ V^{(k)}_{\beta\alpha} & 0 & V^{(k)}_{\beta\gamma} & \\ V^{(k)}_{\gamma\alpha} & V^{(k)}_{\gamma\beta} & 0 & \\ \vdots & & & \ddots \end{pmatrix}, \tag{18}$$

$$Y'_k = \begin{pmatrix} 0 & U^{(k)}_{\alpha\beta} & U^{(k)}_{\alpha\gamma} & \cdots \\ U^{(k)}_{\beta\alpha} & 0 & U^{(k)}_{\beta\gamma} & \\ U^{(k)}_{\gamma\alpha} & U^{(k)}_{\gamma\beta} & 0 & \\ \vdots & & & \ddots \end{pmatrix}, \tag{19}$$

$$Z = \begin{pmatrix} \varepsilon_\alpha & 0 & 0 & \cdots \\ 0 & \varepsilon_\beta & 0 & \\ 0 & 0 & \varepsilon_\gamma & \\ \vdots & & & \ddots \end{pmatrix}. \tag{20}$$

After solving the eigenvalue problem (9), the time-averaged transition probability between the levels can be computed from the quasienergy eigenvectors:

$$\overline{P}_{\alpha\to\beta} = \sum_{l,n,m} \sum_{\gamma} \sum_{l',n',m'} |\langle \beta l n m | \lambda_{\gamma l' n' m'} \rangle \langle \lambda_{\gamma l' n' m'} | \alpha 000 \rangle|^2. \tag{21}$$

The maximum values of 1/2 are reached at the avoided crossings of quasienergies that are associated with multiphoton resonance transitions [26,29,32], and the induced dipole moment can be expanded:

$$\mathbf{d}(t) = \sum_{l,n,m} \mathbf{d}_{l,n,m} e^{-i(l\omega_0 + n\Omega_0 + m\omega_r)t}. \tag{22}$$

Given values of l, n, and m, the angular frequency ω is determined by $\omega = l\omega_0 + n\Omega_0 + m\omega_r$. The harmonic generation spectra in the length form can be expressed by

$$\begin{aligned} S(\omega) &= \frac{4}{6\pi c^3} |\mathbf{d}_{l,n,m}|^2 \\ &= \frac{4}{6\pi c^3} |\sum_{\alpha,\beta} \sum_{l',n',m'} \langle \lambda_{\alpha,l'-l,n'-n,m'-m} | \mu_z | \lambda_{\beta,l',n',m'} \rangle|^2. \end{aligned} \tag{23}$$

III. RESULTS AND DISCUSSIONS

In this section, we present a case study of the multiphoton resonance enhancement of a two-level system driven by two frequency-comb laser fields. The parameters of the fundamental frequency-comb field are peak intensity 2.5×10^{15} W cm^{-2}, carrier frequency 374.7 THz (corresponding to $\omega_c = 0.056954$ a.u. and wavelength 800 nm), and repetition frequency 10 THz (corresponding to $\omega_r = 1.51983 \times 10^{-3}$ a.u. and pulse separation $\tau = 0.1$ ps) generated from a train of Gaussian pulses with 20-fs full width at half maximum (FWHM). The control frequency-comb field is with the peak intensity 1×10^{14} W cm^{-2}, which is 4% of the fundamental field, and its carrier frequency is 749.4 THz, i.e., the second harmonic of the fundamental field. The control field is also generated from a train of Gaussian pulses with 20-fs FWHM, which has repetition frequency 10 THz. For the two-level system, the energy separation between levels is $\hbar\omega_{\alpha\beta} = \varepsilon_\beta - \varepsilon_\alpha = 0.28$ a.u., corresponding to the five-photon dominant resonance regime of the fundamental field ($5\omega_c \approx \omega_{\alpha\beta}$), and the transition dipole moment $\langle \alpha | \mu_z | \beta \rangle = 0.1$ a.u. is used.

The quasiperiodic structure of the quasienergy levels can be represented by

$$\lambda_{\gamma lnm} = \lambda_\gamma + l\omega_0 + n\Omega_0 + m\omega_r, \tag{24}$$

where λ_γ are the eigenvalues of Eq. (9) and l, n, and m are integers. Since $\omega_0 = \omega_\delta + m_1\omega_r$ and $\Omega_0 = \omega'_\delta + m_2\omega_r$, Eq. (24) can be rewritten as

$$\lambda_{\gamma lnm} = \lambda_\gamma + l\omega_\delta + n\omega'_\delta + k\omega_r, \tag{25}$$

where $k = lm_1 + nm_2 + m$. The harmonic radiation can be understood as the dipole transition between quasienergy levels. Then the dipole transition between $\lambda_{\gamma lnm}$ and $\lambda_{\gamma l'n'm'}$ can give rise to the harmonic photon with frequency

$$\omega = (l - l')\omega_\delta + (n - n')\omega'_\delta + (m - m')\omega_r, \tag{26}$$

where $(l - l') + (n - n')$ is odd obeying the dipole transition rule. When the two-level system is driven by the fundamental field alone, only odd harmonics are produced due to the inversion symmetry (red dashed line in Fig. 1). After the employment of the second-harmonic control field, both even and odd harmonics are produced and the intensities of higher-order harmonics are greatly enhanced, as presented in Fig. 1.

Now we explore the optimization of the multiphoton resonance processes by tuning the CEP shifts, $\Delta\phi$ and $\Delta\phi'$. When the two-level system is driven by the fundamental field alone, the multiphoton resonance can be achieved five times by varying $\Delta\phi$, and these five peaks are separated by $2\pi/5$ exactly, as presented by the red dotted line in Fig. 2(a), while for the case of the two-level system driven

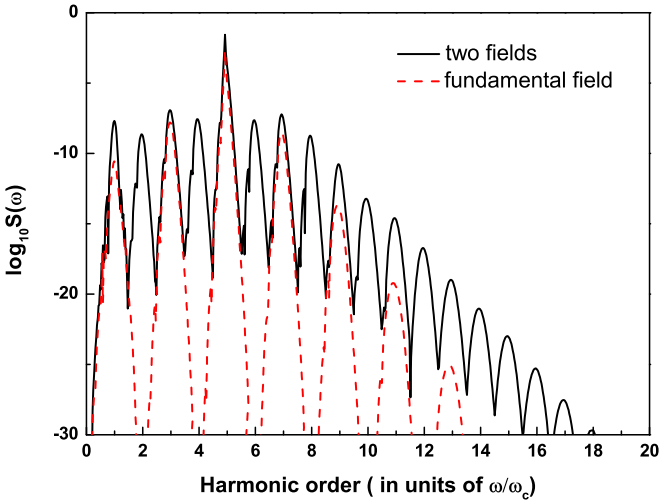

FIG. 1. (Color online) HHG power spectra of the two-level system driven by two fields (black solid line) and the fundamental field alone (red dashed line). Each harmonic has a nested comb structure and all comb peaks are connected by a line. The parameters of the fundamental frequency-comb field are peak intensity $I_f = 2.5 \times 10^{15}$ W cm^{-2}, carrier frequency 374.7 THz, and repetition frequency 10 THz of 20-fs FWHM Gaussian pulses. The parameters of the control frequency-comb field are peak intensity $I_c = 1 \times 10^{14}$ W cm^{-2}, carrier frequency 749.4 THz, and repetition frequency 10 THz of 20-fs FWHM Gaussian pulses. For the case with two driving fields, the CEP shifts are set as $\Delta\phi/2\pi = \Delta\phi'/4\pi = 0.099675$, and for the case with the fundamental fields alone the CEP shift is set as $\Delta\phi/2\pi = 0.098575$.

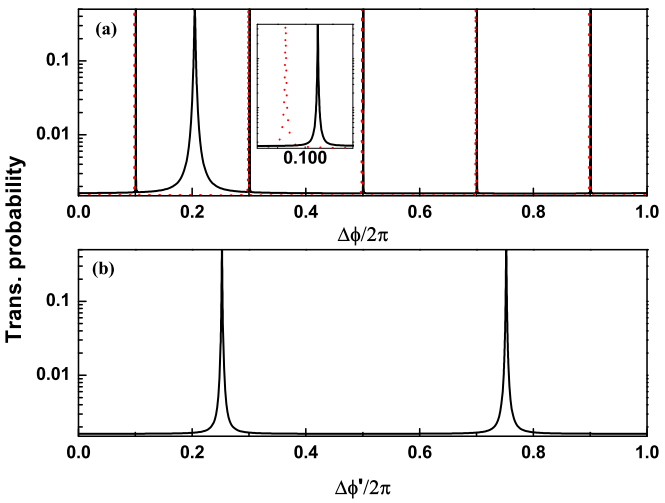

FIG. 2. (Color online) (a) and (b) Time-averaged transition probabilities for the two-level system driven by two frequency-comb laser fields as a function of the CEP shift of the fundamental and control fields, $\Delta\phi$ and $\Delta\phi'$, respectively. In (a) $\Delta\phi$ is varied with fixed $\Delta\phi'/2\pi = 0.15$, and in (b) $\Delta\phi'$ is varied with fixed $\Delta\phi/2\pi = 0$. As a comparison, the transition probabilities for the two-level systems driven by the fundamental field alone are presented with a red dotted line in (a). Inset: The enlarged plot of the transition probabilities around $\Delta\phi/2\pi = 0.1$. The other laser parameters are the same as those in Fig. 1.

by both the fundamental and control fields Fig. 2(a) shows the time-averaged transition probabilities as a function of $\Delta\phi$ with fixed $\Delta\phi'/2\pi = 0.15$. With the coupling of the control field, the five resonant peaks are shifted due to the ac Stark effect, and one more resonance peak appears around $\Delta\phi/2\pi = 0.2$. Meanwhile, Fig. 2(b) presents the time-averaged transition probabilities of the two-level system driven by two fields as a function of $\Delta\phi'$ with fixed $\Delta\phi/2\pi = 0$, the multiphoton resonance is achieved two times by varying $\Delta\phi'$, and the two resonance peaks are separated by π exactly. The additional resonance peak in Fig. 2(a) and the two peaks in Fig. 2(b) indicate the existence of the three-photon-resonant transition paths involving one fundamental-field photon and two control-field photons.

The n-photon resonance condition for the case of the system driven by two frequency-comb fields shall be recast as

$$\omega_{\rm res} \equiv n_1\omega_\delta + n_2\omega'_\delta \pmod{\omega_r}, \tag{27}$$

where $\omega_{\rm res}$ is the resonance frequency, $\omega_\delta = \Delta\phi/\tau$, and $\omega'_\delta = \Delta\phi'/\tau$ are offsets of the fundamental and control fields, respectively. Equation (27) means the remainders of $\omega_{\rm res}$ and $n_1\omega_\delta + n_2\omega'_\delta$ are the same when divided by ω_r. If no control-field photon is involved in the multiphoton transition process, i.e., $n_2 = 0$, Eq. (27) is recovered to

$$\omega_{res} \equiv n\omega_\delta \pmod{\omega_r}, \tag{28}$$

which is the n-photon resonance condition for one driving frequency-comb field [26,32,33]. Odd n equal-spacing multiphoton resonance peaks are reached by tuning $\Delta\phi$. On the other hand, if control-field photons are involved, the resonance condition (27) can be satisfied by tuning $\Delta\phi$ ($\Delta\phi'$) with fixed $\Delta\phi'$ ($\Delta\phi$). For instance, with fixed $\Delta\phi'/2\pi = 0.15$, Eq. (27) is satisfied when $n_1 = 1$, $n_2 = 2$, and $\Delta\phi/2\pi = 0.204570$, while with fixed $\Delta\phi/2\pi = 0$ Eq. (27) is satisfied when $n_1 = 1$, $n_2 = 2$, and $\Delta\phi'/2\pi = 0.252383$ and 0.752383, agreeing with the additional peak in Fig. 2(a) and the two peaks in Fig. 2(b).

Generally, each quasienergy level is populated via a single multiphoton-transition path, and the level energy is dependent on the offset frequencies of the two frequency-comb fields. As a result, dipole transitions between quasienergy levels produce harmonic-comb elements with different absolute frequencies which are dependent on the offset frequencies. In particular, different combinations of frequencies can lead to the final quasienergy levels with the same energy, i.e., the same final quasienergy level, when the two CEP shifts fulfill the specific matching condition. Then the quasienergy level can be populated via different multiphoton transition paths, and the superposition of these paths provides an approach to coherently control the quasienergy level, as well as the HHG spectra [34]. In our case of the two-level system driven by the fundamental- and second-harmonic fields, the matching condition for the superposition of paths is

$$\omega'_\delta = 2\omega_\delta, \quad \text{or} \quad \Delta\phi' = 2\Delta\phi. \tag{29}$$

Then the frequency

$$\begin{aligned}\Omega_0 &= m_2\omega_r + \omega'_\delta \\ &= (m_2 - 2m_1)\omega_r + 2(m_1\omega_r + \omega_\delta) \\ &= 2\omega_0 + m_\delta\omega_r\end{aligned} \tag{30}$$

with $m_\delta = m_2 - 2m_1$ is dependent on ω_0 and ω_r. The number of independent frequencies is reduced from 3 to 2, and the total Hamiltonian can be rewritten as

$$H(\mathbf{r},t) = \hat{H}_0(\mathbf{r}) - \sum_{k=-N}^{N} \frac{1}{2}\mu_z E_k [e^{i(\omega_0+k\omega_r)t} + e^{-i(\omega_0+k\omega_r)t}] - \sum_{k=-N'}^{N'} \frac{1}{2}\mu_z E'_k [e^{i(2\omega_0+k'\omega_r)t} + e^{-i(2\omega_0+k'\omega_r)t}], \tag{31}$$

in which $k' = k + m_\delta$. The Floquet matrix H_F can be reconstructed by

$$\langle \alpha l m | H_F | \beta l' m' \rangle = H_{\alpha\beta}^{[l-l',m-m']} + (l\omega_0 + m\omega_r)\delta_{\alpha,\beta}\delta_{l,l'}\delta_{m,m'}, \tag{32}$$

with

$$H_{\alpha,\beta}^{[l-l',m-m']} = \varepsilon_\alpha \delta_{\alpha,\beta}\delta_{l,l'}\delta_{m,m'} + \sum_{k=-N}^{N} V_{\alpha,\beta}^{(k)}(\delta_{l+1,l'}\delta_{m+k,m'} + \delta_{l-1,l'}\delta_{m-k,m'}) + \sum_{k=-N'}^{N'} U_{\alpha,\beta}^{(k)}(\delta_{l+2,l'}\delta_{m+k',m'} + \delta_{l-2,l'}\delta_{m-k',m'}). \tag{33}$$

The harmonic generation spectra can be recast by

$$S(\omega) = \frac{4}{6\pi c^3}|\mathbf{d}_{l,m}|^2 = \frac{4}{6\pi c^3}\left|\sum_{\alpha,\beta}\sum_{l',m'}\langle \lambda_{\alpha,l'-l,m'-m}|\mu_z|\lambda_{\beta,l',m'}\rangle\right|^2, \tag{34}$$

in which $\omega = l\omega_0 + m\omega_r$.

Under the matching condition, we first investigate the enhancement of HHG power spectra via multiphoton resonance by tuning the CEP shifts and peak intensities of the frequency-comb fields. In Fig. 3(a), we present the time-averaged transition probabilities as a function of $\Delta\phi$ with $\Delta\phi' = 2\Delta\phi$ and peak intensities of the fundamental and control fields, $I_f = 2.5 \times 10^{15}$ W cm^{-2} and $I_c = 1 \times 10^{14}$ W cm^{-2}, respectively. Resonance peaks of different multiphoton transition paths are coincident due to the superposition of transition paths. As a result, there are only five resonance peaks in the plot. Figure 3(b) shows the enhancement of HHG by varying $\Delta\phi/2\pi = \Delta\phi'/4\pi = 0$ (off resonance), 0.09, and 0.099675 (near resonance). Both even and odd harmonics can be enhanced via multiphoton resonance which can be achieved by varying CEP shifts. Table I lists the power spectrum values of the maximum peak for the near- and off-resonance cases with several control-field peak intensities. For the case of control-field peak intensity $I_c = 1 \times 10^{12}$ W cm^{-2}, the HHG power spectra are enhanced by about 10^8 times when the multiphoton resonance is achieved. For the case of $I_c = 1 \times 10^{13}$ W cm^{-2}, the enhancement factor via multiphoton resonance is about 10^7 times, while for the case of $I_c = 1 \times 10^{14}$ W cm^{-2} it is about 10^6 times. On the other hand, the HHG power spectra

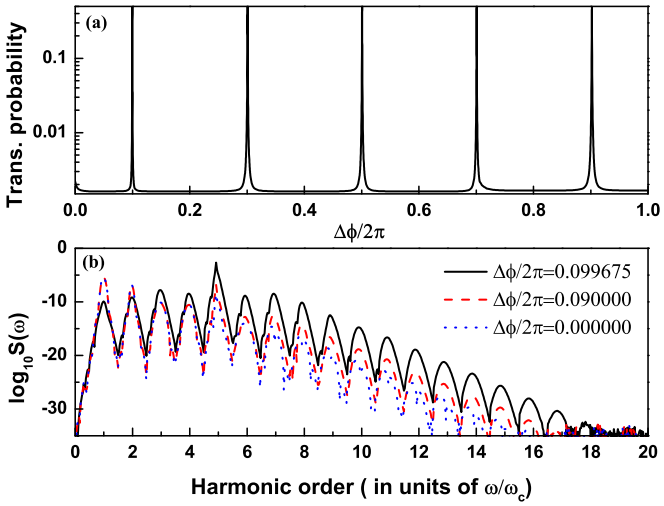

FIG. 3. (Color online) (a) Time-averaged transition probabilities for the two-level system driven by two frequency-comb laser fields as a function of the CEP shift of the fundamental field, $\Delta\phi$, while keeping $\Delta\phi' = 2\Delta\phi$. (b) Enhancement of HHG by varying the CEP shifts. For clarity, HHG peaks of the comb structure are connected by a line. The laser parameters are the same as those in Fig. 1.

can be enhanced by increasing I_c. For instance, with the increase of I_c from 1×10^{12} to 1×10^{14} W cm^{-2}, the harmonic orders $n > 8$ are enhanced by about 10^3 times for both off- and near-resonance cases. Note that the multiphoton resonant condition is dependent on the peak intensity of the control frequency-comb field. Thus it provides a route to achieve multiphoton resonance with fixed absolute comb frequencies, by varying the peak intensity of the control field.

When the matching condition is satisfied, the same final quasienergy level can be populated via different multiphoton transition paths. For example, the quasienergy level $\lambda_{\gamma,l',m'} = \lambda_\gamma + l'\omega_0 + m'\omega_r$ can be populated from $\lambda_{\gamma,l'-1,m'-k} = \lambda_\gamma + (l'-1)\omega_0 + (m'-k)\omega_r$ by absorbing a fundamental-field photon $\omega_0 + k\omega_r$, as well as from $\lambda_{\gamma,l'-2,m'-k} = \lambda_\gamma + (l'-2)\omega_0 + (m'-k)\omega_r$ by absorbing a second-field photon $\Omega_0 + (k - m_\delta)\omega_r$. Thus the quasienergy level, as well as the HHG power spectra, can be coherently modulated via destructive or constructive interference of multiphoton-transition paths. The interference can be controlled by varying the relative phase φ between fields, with which the fundamental- and second-harmonic fields are defined as

$$E(t) = \sum_n f(t - n\tau)e^{i(\omega_c t - n\omega_c\tau + n\Delta\phi)} + \text{c.c.} \tag{35}$$

and

$$E'(t) = \sum_n f'(t - n\tau)e^{i(\Omega_c t - n\Omega_c\tau + n\Delta\phi' + \varphi)} + \text{c.c.}, \tag{36}$$

respectively. Consequently the total electric field shall be written as

$$E_t(t) = \sum_{k=-N}^{N} E_k e^{i\omega_k t} + \sum_{k=-N'}^{N'} E'_k e^{i\Omega_k t}e^{i\varphi} + \text{c.c.}, \tag{37}$$

TABLE I. Effects on the power spectra by varying the CEP shifts $\Delta\phi' = 2\Delta\phi$ under different control-field peak intensities. n is the harmonic order of the maximum peak for each harmonic and $S(n\omega_c)$ is the corresponding HHG power spectrum values at $\omega = n\omega_c$. The label A indicates the near-resonance cases: $\Delta\phi/2\pi = \Delta\phi'/4\pi = 0.098586$, 0.098685, and 0.099675 corresponding to the control-field peak intensities $I_c = 1\times10^{12}$, 1×10^{13}, and 1×10^{14} W cm^{-2}, respectively, while B indicates the off-resonance cases with $\Delta\phi/2\pi = 0$. The numbers in brackets indicate the power of 10. The other laser parameters are the same as those in Fig. 1.

1×10^{12} W/cm^2				1×10^{13} W/cm^2				1×10^{14} W/cm^2			
A		B		A		B		A		B	
n	$S(n\omega_c)$	n	$S(n\omega_c)$	n	$S(n\omega_c)$	n	$S(n\omega_c)$	n	$S(n\omega_c)$	n	$S(n\omega_c)$
4.92	2.15[−03]	4.91	1.04[−10]	4.92	2.15[−03]	4.94	3.13[−12]	4.92	2.14[−03]	4.91	3.23[−09]
5.94	1.40[−11]	5.95	9.24[−17]	5.94	1.40[−11]	5.92	8.94[−16]	5.94	1.40[−09]	5.87	8.37[−15]
6.93	3.41[−9]	6.86	6.19[−17]	6.93	3.41[−9]	7.02	1.65[−15]	6.93	3.41[−09]	6.86	2.42[−15]
7.92	7.41[−13]	7.98	1.42[−20]	7.92	7.41[−13]	7.98	7.62[−20]	7.92	7.41[−11]	7.85	4.77[−17]
8.91	2.22[−14]	8.81	3.13[−22]	8.91	2.22[−14]	8.99	2.62[−22]	8.91	3.08[−13]	8.83	2.33[−19]
9.90	1.69[−17]	9.79	1.75[−25]	9.90	1.69[−17]	9.98	1.23[−24]	9.90	1.78[−15]	9.82	1.11[−21]
10.89	8.76[−20]	10.75	9.99[−28]	10.89	8.76[−20]	10.97	4.23[−27]	10.89	2.41[−17]	10.78	1.31[−23]
11.88	1.14[−22]	11.74	1.10[−30]	11.88	1.14[−22]	11.95	1.27[−29]	11.88	1.27[−19]	11.77	7.18[−26]

the total Hamiltonian (31) can be rewritten as

$$H(\mathbf{r},t) = \hat{H}_0(\mathbf{r}) - \sum_{k=-N}^{N}\frac{1}{2}\mu_z E_k[e^{i(\omega_0+k\omega_r)t} + e^{-i(\omega_0+k\omega_r)t}] - \sum_{k=-N'}^{N'}\frac{1}{2}\mu_z E'_k[e^{i(2\omega_0+k'\omega_r)t}e^{i\varphi} + e^{-i(2\omega_0+k'\omega_r)t}e^{-i\varphi}], \tag{38}$$

and the Floquet matrix H_F is constructed by

$$\langle\alpha lm|H_F|\beta l'm'\rangle = H_{\alpha\beta}^{[l-l',m-m']} + (l\omega_0 + m\omega_r)\delta_{\alpha,\beta}\delta_{l,l'}\delta_{m,m'}, \tag{39}$$

with

$$H_{\alpha,\beta}^{[l-l',m-m']} = \varepsilon_\alpha\delta_{\alpha,\beta}\delta_{l,l'}\delta_{m,m'} + \sum_{k=-N}^{N} V_{\alpha,\beta}^{(k)}(\delta_{l+1,l'}\delta_{m+k,m'} + \delta_{l-1,l'}\delta_{m-k,m'}) + \sum_{k=-N'}^{N'} U_{\alpha,\beta}^{(k)}(\delta_{l+2,l'}\delta_{m+k',m'}e^{i\varphi} + \delta_{l-2,l'}\delta_{m-k',m'}e^{-i\varphi}). \tag{40}$$

Then the eigenvectors and induced dipole moment matrix elements $\mathbf{d}_{l,m}$ are complex; they can be modulated by tuning the relative phase φ between fields, resulting in the coherent control of the harmonic spectrum. In the near-resonance case of the two-level system driven by fundamental and control fields with CEP shifts $\Delta\phi/2\pi = \Delta\phi'/4\pi = 0.099675$ and peak intensities 2.5×10^{15} and 1×10^{14} W cm^{-2}, respectively, we calculate the HHG spectra as a function of the relative phase φ between fields and take the peak elements for the fifth and eighth harmonics as examples to investigate the coherent control of HHG power spectra. In Fig. 4(a), we plot the normalized intensities of the peak elements for the fifth and eighth harmonics as a function of the relative phase φ. Interference between different multiphoton resonant-transition paths occurs and both intensities oscillate with a modulation period of π. On the other hand, Fig. 4(b) shows that the phases of the peak elements present quite different modulation behaviors while varying the relative phase φ. For the peak in the fifth harmonic, the phase of $\mathbf{d}_{l,m}$ oscillates around π, while for the peak in the eighth harmonic the phase of $\mathbf{d}_{l,m}$ oscillates from π to $-\pi$. The calculation results of all comb elements in odd and even harmonics, which are not presented in the paper, oscillate with the same modulation period, and their oscillation features are similar to those of the peak elements in fifth and eighth harmonics, respectively.

IV. CONCLUSION

In conclusion, we present a theoretical investigation of multiphoton resonance dynamics of a two-level system driven by two frequency-comb fields with carrier frequencies ω_c

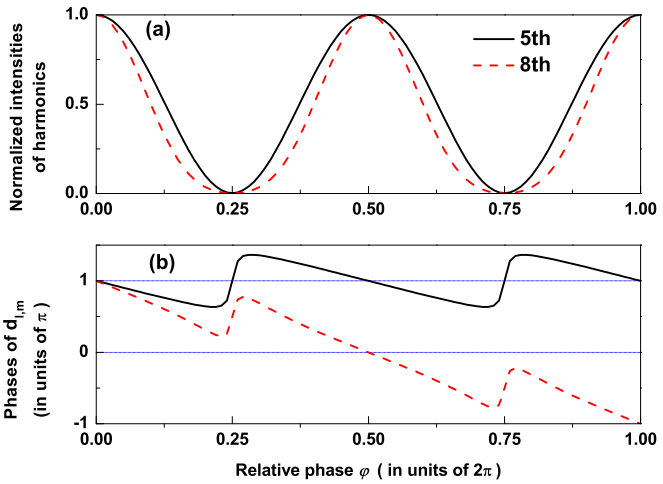

FIG. 4. (Color online) (a) The normalized intensities and (b) the phases of the peak elements for the fifth (black solid line) and eighth (red dashed line) harmonics as a function of the relative phase φ between fundamental- and second-harmonic fields. $\Delta\phi/2\pi = \Delta\phi'/4\pi = 0.099675$ are set for the achievement of multiphoton resonance. Other parameters are the same as those in Fig. 1.

and $\Omega_c = 2\omega_c$. Many-mode Floquet theory is employed for accurate treatment of the interaction between a quantum system and the frequency-comb fields. With the coupling of the second-harmonic control frequency-comb field, even-order harmonics are generated due to the coupling of the second-harmonic frequency-comb field. Our calculation shows that the HHG power spectra can be multiphoton-resonantly enhanced by tuning the CEP shifts and peak intensities of the frequency-comb fields. Furthermore, additional multiphoton transitions involving photons from both of the two fields occur, leading to the emission of the harmonic comb element with frequency dependent on both $\Delta\phi$ and $\Delta\phi'$. We found that different multiphoton transition paths can interfere with each other when the matching condition is fulfilled, and the superposition of paths allows the coherent control of the frequency-comb structure in harmonics by varying the relative phase between two fields.

This two-frequency-comb-fields approach provides alternative routes for the optimal control of the frequency-comb structures. For instance, with fixed peak intensities of the frequency-comb fields, the HHG power spectra can be enhanced via multiphoton resonance by tuning the CEP shifts, while for the achievement of comb elements with desired absolute frequencies the CEP shifts are fixed and the multiphoton-resonant enhancement can be achieved by tuning peak intensities of the frequency-comb fields. At the same time, the CEP shifts of driving and control fields can be matched to realize the superposition of different multiphoton-transition paths, without the break of resonant conditions. The superposition allows us to coherently control the HHG power spectra via destructive or constructive interference of multiphoton-transition paths. In addition, it also provides a possible way to study the multiphoton transition processes, by observing the amplitudes of comb elements generated via different multiphoton-transition paths, and the multiphoton-transition paths can be identified by the absolute frequencies of comb elements, with the help of the known CEP shifts of fields.

ACKNOWLEDGMENTS

This work was supported by the Natural Science Foundation of China (Grants No. 11374239, No. 21203144, and No. 11074199), Doctoral Fund of Ministry of Education of China (Grant No. 20120201120056), and the Fundamental Research Funds for the Central Universities.

[1] H. S. Margolis *et al.*, Science **306**, 1355 (2004).
[2] A. Marian, M. C. Stowe, D. Felinto, and J. Ye, Phys. Rev. Lett. **95**, 023001 (2005).
[3] J. E. Stalnaker, Y. LeCoq, T. M. Fortier, S. A. Diddams, C. W. Oates, and L. Hollberg, Phys. Rev. A **75**, 040502 (2007).
[4] R. Holzwarth, T. Udem, T. W. Hänsch, J. C. Knight, W. J. Wadsworth, and P. S. J. Russell, Phys. Rev. Lett. **85**, 2264 (2000).
[5] M. Niering *et al.*, Phys. Rev. Lett. **84**, 5496 (2000).
[6] M. Fischer *et al.*, Phys. Rev. Lett. **92**, 230802 (2004).
[7] V. A. Dzuba and V. V. Flambaum, Phys. Rev. A **61**, 034502 (2000).
[8] M. Herrmann *et al.*, Phys. Rev. A **79**, 052505 (2009).
[9] D. Z. Kandula, C. Gohle, T. J. Pinkert, W. Ubachs, and K. S. E. Eikema, Phys. Rev. Lett. **105**, 063001 (2010).
[10] H. Mabuchi, J. Ye, and H. J. Kimble, Appl. Phys. B **68**, 1095 (1999).
[11] E. E. Eyler *et al.*, Euro. Phys. J. D **48**, 43 (2008).
[12] M. Takamoto, F. L. Hong, R. Higashi, and H. Katori, Nature (London) **435**, 321 (2005).
[13] S. A. Diddams *et al.*, Science **293**, 825 (2001).
[14] E. Peik and Chr. Tamm, Europhys. Lett. **61**, 181 (2003).
[15] W. G. Rellergert, D. DeMille, R. R. Greco, M. P. Hehlen, J. R. Torgerson, and E. R. Hudson, Phys. Rev. Lett. **104**, 200802 (2010).
[16] C. J. Campbell, A. G. Radnaev, and A. Kuzmich, Phys. Rev. Lett. **106**, 223001 (2011).
[17] V. Gerginov, C. E. Tanner, S. A. Diddams, A. Bartels, and L. Hollberg, Opt. Lett. **30**, 1734 (2005).
[18] Th. Udem, R. Holzwarth, and T. W. Hänsch, Nature (London) **416**, 233 (2002).
[19] S. T. Cundiff and J. Ye, Rev. Mod. Phys. **75**, 325 (2003).
[20] C. Gohle *et al.*, Nature (London) **436**, 234 (2005).
[21] R. J. Jones, K. D. Moll, M. J. Thorpe, and J. Ye, Phys. Rev. Lett. **94**, 193201 (2005).
[22] A. Cingöz *et al.*, Nature (London) **482**, 68 (2012).
[23] J. J. Carrera, S.-K. Son, and Shih-I Chu, Phys. Rev. A **77**, 031401(R) (2008).
[24] J. J. Carrera and Shih-I Chu, Phys. Rev. A **79**, 063410 (2009).
[25] D. C. Yost *et al.*, Nat. Phys. **5**, 815 (2009).
[26] Sang-Kil Son and Shih-I Chu, Phys. Rev. A **77**, 063406 (2008).
[27] Shih-I Chu and D. A. Telnov, Phys. Rep. **390**, 1 (2004).
[28] T. S. Ho, Shih-I Chu, and J. V. Tietz, Chem. Phys. Lett. **96**, 464 (1983).
[29] T.-S. Ho and Shih-I Chu, J. Phys. B **17**, 2101 (1984).
[30] T.-S. Ho and Shih-I Chu, Phys. Rev. A **31**, 659 (1985).
[31] T.-S. Ho and Shih-I Chu, Phys. Rev. A **32**, 377 (1985).
[32] Di Zhao, Fu-li Li, and Shih-I Chu, Phys. Rev. A **87**, 043407 (2013).
[33] Di Zhao, Fu-li Li, and Shih-I Chu, J. Phys. B **46**, 145403 (2013).
[34] D. A. Telnov, J. Wang, and Shih-I Chu, Phys. Rev. A **52**, 3988 (1995).